Lack of the Flavin-Containing Monooxygenase FmoA Partially Impairs the Symbiotic Interaction of Mesorhizobium Huakuii with Astragalus Sinicus

Hetao Wu
South-Central University for Nationalities
Qian Zou
South-Central University for Nationalities
Sha Luo
South-Central University for Nationalities
Donglan He
South-Central University for Nationalities
Xiaohua Li
South-Central University for Nationalities
Chunlan Yan
South-Central University for Nationalities
Guojun Cheng (chengguojun@mail.scuec.edu.cn)
South-Central University for Nationalities https://orcid.org/0000-0002-5921-4543

Research article

Keywords: Mesorhizobium huakuii, FmoA, Antioxidant function, Symbiosis nitrogen fixation, RNA-Seq analysis of nodule bacteroids

Posted Date: May 19th, 2020

DOI: https://doi.org/10.21203/rs.3.rs-27635/v1

Abstract

Background: Flavin-containing monooxygenases (FMOs) catalyze the NADPH-dependent N- or S-oxygenation of numerous foreign chemicals, and thus may mediate interactions between microorganisms and their chemical environment. The aim of this study was to investigate the role of FMO in symbiotic nitrogen fixation of *Mesorhizobium huakuii* and its host plant *Astragalus sinicus.*

Results: A mutation in *M. huakuii fmoA* gene was generated by homologous recombination. The *fmoA* mutant grew more slowly than its parental strain, and displayed decreased antioxidative capacity under higher concentration of H_2O_2 and cumene hydroperoxide (CUOOH), indicating that FmoA plays an important role in response to the peroxides. The *fmoA* mutant strain displayed no difference of peroxidase activity and glutathione reductase activity, but significantly lower level of glutathione and hydrogen peroxide content than the wild type. Real-time quantitative PCR showed that the *fmoA* gene expression is significantly up-regulated in three different stages of nodule development. The *fmoA* mutant was severely impaired in its rhizosphere colonization, and its symbiotic properties in *Astragalus sinicus* were drastically affected. Transcriptomes in root-nodule bacteroids were analyzed and compared. A total of 1233 genes were differentially expressed, of which 560 were up-regulated and 673 were down-regulated in HKfmoA bacteroids compared with that in 7653R bacteroids. The transcriptomic data allowed us to determine additional target genes, whose differential expression was able to explain the observed the changes of symbiotic phenotype in the mutant-infected nodules.

Conclusions: The *fmoA* gene is essential for antioxidant capacity and symbiotic nitrogen fixation. Furthermore, RNA-Seq based global transcriptomic analysis provided a comprehensive view of *M. huakuii fmoA* gene involved in nodule senescence and symbiotic nitrogen fixation.

Background

Mesorhizobium huakuii is an aerobic, motile, Gram-negative, non-spore-forming rod bacterium that can exist as a soil saprophyte or as an effective nitrogen-fixing microsymbiont of the legume *Astragalus sinicus.* Strains of *M. huakuii* could only effectively nodulate and efficiently fix nitrogen on its original host plant, which makes it a very significant material. The establishment of the nitrogen-fixing symbiosis between rhizobia and legumes requires a mutual exchange of signal molecules between the two partners [1]. The biosynthesis of Nod factors is specific to rhizobial species and is induced by flavonoids, excreted by the host plant [2]. Rhizobia are able to enter the plant root through an infection thread or a more primitive way called intercellular invasion, penetrate into the root cortex and spread inside nodules [3]. Nodules are complex structures containing a combination of infected and non-infected plant cells. Infected cells are filled with numerous symbiosomes containing nitrogen-fixing bacteroids [4]. The nitrogenase, which is responsible for nitrogen reduction, is extremely sensitive to oxygen, therefore, this process requires conditions that are anoxic or nearly anoxic [5]. In addition to reducing N_2 and protons, nitrogenase can reduce a number of small, non-physiological substrates including a wide array of carbon-containing compounds [6]. At the early stage of *M. huakuii-A. sinicus* symbiosis, reactive oxygen species

(ROS) are produced in plant defense response against Rhizobia, and are involved in the control of infection and nodulation [7]. Superoxide radicals and hydrogen peroxide have been detected in infection threads. In addition, there is also evidence that nitric oxide exists in the nodules [8]. Iron metabolism, monooxygenases, and secondary metabolism appeared to participate in oxidative responses [9].

Flavin-containing monooxygenases (EC 1.14.13.8) (FMOs) catalyze the NADPH-dependent N- or S-oxygenation of nucleophilic nitrogen, sulfur, and phosphorous atoms in various drugs, pesticides, and xenobiotics [10]. In the presence of O_2, FMOs involve the formation of 4a-hydroperoxy-FAD (FAD-OOH) intermediate, in which a new center of chirality is created at the 4a position during the enzymatic reactions [11]. In such a reaction, one atom of molecular oxygen is incorporated into the carboxylic acid group, and the other oxygen atom is incorporated into water [12]. FMOs are enzymes belonging to the "Class B" of flavin monooxygenases, together with N-hydroxylating monooxygenases (NMOs) and Baeyer–Villiger monooxygenases (BVMOs) [13]. This class of FMOs has characteristic conserved sequence motifs, and displays relaxed coenzyme specificity by accepting both reduced form of nicotinamide adenine dinucleotide (NADH) and reduced nicotinamide adenine dinucleotide phosphate (NADPH), as a coenzyme, which is a novel and attractive feature among biocatalysts capable of catalyzing Baeyer-Villiger oxidations [14, 15].

FMOs in eukaryotes have been exploited as diverse biocatalysts, and have been well studied in detail [16]. The best known example of eukaryotic FMO is probably from mammals, where FMO3 is an important hepatic enzyme for the detoxification of xenobiotics including trimethylamine (TMA) [17, 18]. Plant FMOs are essential for the initiate systemic accumulation of salicylic acid and systemic defense responses provoked by the virulent strains [19]. In yeast, FMOs are required for cell growth under reductive stress and involved in the maintenance or regulation of intracellular reducing potential [20]. FMOs are also present in *E. coli*, and the presence of FMO were detected in many bacterial genomes. However, the physiological role of bacterial FMOs has thus far not been known [18].

The functions of the flavin-containing monooxygenases are of interest not only because they oxidatively metabolizes a wide variety of nitrogen, sulfur-, and phosphorous-containing xenobiotics, but also because they appear to share various functions in protecting organisms against ROS and detoxifying xenobiotics. Here, we identified a FMO gene *fmoA* in *M. huakuii* 7653R, and the roles of *M. huakuii* FmoA in free-living bacteria and during N-fixing symbiosis with *A. sinicus* were investigated by analyzing the phenotypes of a *fmoA* mutant strain. A transcriptome analysis was also carried out to discover clues that might explain the differences in the nodules induced by the *fmoA* mutant and the wild type strain.

Results

Construction of *M. huakii fmoA* mutant

The gene MCHK_8187 in *M. huakuii*, encoding a flavin-dependent oxidoreductase (FmoA), is expressed at high levels in the nodule during plant symbiosis. *fmoA* gene is predicted to encode a 350-amino acid

polypeptide with an expected molecular mass of 39.4 kDa and a pI value of 5.85. To confirm the function of the *fmoA* gene in growth, antioxidation capacity and symbiotic nitrogen fixation, we constructed its mutant HKfmoA by a single crossover homologous recombination. In liquid AMS minimal medium with NH_4Cl as nitrogen source and glucose as carbon source, HKfmoA grew more slowly than the parent strain 7653R (Fig. 1). The growth of HKfmoA in AMS media with glucose as sole carbon source was restored by complementation with *fmoA* carried on a plasmid (pBBRfmoA) (Fig. 1).

Antioxidation analysis of *M. huakii fmoA* mutant

To investigate the role of FmoA in protection against oxidative stress, survival assays were carried out to determine the capacity of the mutant HKfmoA to oxide hydrogen peroxide (H_2O_2) and organic oxide cumene hydroperoxide (CUOOH). The survival rates of HKfmoA were not significantly affected by the presence of the lower concentrations of 1, 5 mmol/L H_2O_2 and 0.1 mmol/L CUOOH, whereas the survival ability of mutant HKfmoA was affected by the treatment with the higher concentrations of 10 mmol/L H_2O_2 and 1, 5 mmol/L CUOOH (Table 1).

Table 1
Tolerance of stains to different concentrations of H_2O_2 and CUOOH

Oxidants	**H_2O_2**			**CUOOH**		
concentration (mmol/L)	1	5	10	0.1	1	5
7653R (CFU/mL)	$(1.07 \pm 0.34) \times 10^9$ a	$(1.01 \pm 0.21) \times 10^9$ a	$(9.17 \pm 0.76) \times 10^8$ a	$(9.93 \pm 2.01) \times 10^8$ a	$(1.30 \pm 0.27) \times 10^8$ a	$(6.93 \pm 0.35) \times 10^6$ a
HKfmoA (CFU/mL)	$(8.50 \pm 1.92) \times 10^8$ a	$(7.63 \pm 2.11) \times 10^8$ a	$(3.38 \pm 0.48) \times 10^8$ b	$(8.87 \pm 1.64) \times 10^8$ a	$(5.10 \pm 0.99) \times 10^7$ b	$(3.43 \pm 0.30) \times 10^6$ b

All data are averages (± SEM) from three independent experiments. [a, b]Values in each column followed by the same letter are not significantly different ($P \leq 0.05$).

It has been reported that the yeast flavin-dependent monooxygenase (yFMO) devotes to the cellular pools of oxidized thiols that, together with GSH from glutathione reductase, create the optimum redox environment of cellular systems [20]. The role of the *M. huakuii* FmoA in the function of regulating the cellular redox environment was investigated by quantifying the peroxidase activity, glutathione reductase activity, hydrogen peroxide content and GSH content in 5 mM H_2O_2-induced oxidative stress conditions. The results showed that the peroxidase activity and glutathione reductase activity in the mutant HKfmoA were not different from that of parent strain 7653R, but its GSH content and hydrogen peroxide content were significantly lower (Table 2). Therefore, FmoA may play important roles in oxidative stress resistance and regulating the cellular redox environment in *M. huakuii*.

Table 2
The enzymatic activities and non-enzymatic antioxidant content of *M. huakuii* strains

Strains *M. huakuii*	Peroxidase activity (U/mg protein)	Glutathione reductase activity(U/mg protein)	Hydrogen peroxide content (uM)	GSH (mmol/10^9 cells)
7653R	1.29 ± 0.215 [a]	0.4 ± 0.008 [a]	3.67 ± 0.018 [a]	0.94 ± 0.016 [a]
HKfmoA	1.70 ± 0.180 [a]	0.47 ± 0.014 [a]	2.39 ± 0.122 [b]	0.47 ± 0.024 [b]

All data are averages (± SEM) from three independent experiments. [a, b]Values in each column followed by the same letter are not significantly different ($P \leq 0.05$).

Rhizosphere colonization by *M. huakuii* strains

Competition between the *fmoA* mutant HKfmoA and parent strain 7653R for growth in the plant rhizosphere was measured by inoculating a low number of *M. huakuii* strains into the *A. sinicus* rhizosphere (10^3 to 10^4 CFU per seedling), and determining the total amount of bacteria after 7 days. When the mutant HKfmoA and the parent 7653R were inoculated alone into short-term colonization of sterile plant rhizosphere, the ratio between mutant HKfmoA and wild-type7653R was 34.4% (Fig. 2). When both strains were inoculated together in equal proportion, mutant HKfmoA was at a significant disadvantage (23.20% of bacteria recovered) compared to the wild type. In the same case, even when mutant HKfmoA was co-inoculated at a 10-fold excess over the wild type 7653R, it still accounted for only 40.33% of bacteria recovered (Fig. 2). Fmos can mediate interactions between microorganisms and their environment, and the present of Fmos in Rhizobium can provide a competitive advantage in competition for survival in the rhizosphere soil. The decreased ability of the *fmoA* mutant to grow in a sterile host plant rhizosphere shows that FmoA is essential for colonization of the host plant rhizosphere by *M. huakuii*.

Effect of mutation of *fmoA* on nodulation

To observe the nodulation characteristics and measure nitrogenase activity of the *fmoA* mutant, *A. sinicus* seedlings were inoculated with *M. huakuii* strains, and,the number, structure, and acetylene reduction activity (ARA) values of the nodules were analyzed 28 days post inoculation (Figure S1). The results showed that there was no statistically significant difference in the number of nodules per plant between plants inoculated strain HKfmoA and plants inoculated with wild-type 7653R (Table 3). A notable feature of our study was that the nitrogen fixation capacity was severely affected in the *fmoA* mutant HKfmoA, with a reduction from 23.42 nmol of C_2H_4 $plant^{-1}$ h^{-1} in 7653R to 7.40 nmol of C_2H_4 $plant^{-1}$ h^{-1} in the mutant (Table 3). Uninoculated controls showed exhibited severe symptoms of nitrogen deficiency. When recombinant plasmid pBBRfmoA was introduced into mutant HKfmoA, plants inoculated with the resulting strain HKfmoA (pBBRfmoA) formed normal nodules (Fig. 3), and there was

no significant difference in nitrogen-fixing ability between 7653R-inoculated plants and HKfmoA-inoculated plants (Table 3). The structural organization of mature root nodules of *A. sinicus* is studied by thin-sectioning and scanning electron microscopy techniques. Microscopic analysis of HKfmoA nodules showed that they were spherical rather than elongated (Fig. 3). Moreover, bacterial size, structure and membrane incrassation, as observed by electronic microscopy of nodule sections, indicated that the fmoA mutant bacteroids had undergone premature senescence (Fig. 3). In addition, poly-b-hydroxibutyrate granules were only detected in the *fmoA* mutant bacteroids".

Table 3

Symbiotic phenotype of 7653R and HKfmoA[α]

Strain *M.huakuii*	Number of total nodules per plant [β]	Acetylene reduction activity (nmol of ethylene/plant/h) [β]	Acetylene reduction activity (nmol of ethylene/nodulet/h) [β]
7653R	11.0 ± 4.36[a]	23.42 ± 0.95 [a]	2.32 ± 0.71 [a]
HKfmoA	12.3 ± 3.79[a]	7.40 ± 2.31 [b]	0.75 ± 0.13[b]
HKllm(pBBRfmoA)	9.7 ± 4.51[a]	20.65 ± 1.72 [a]	2.49 ± 1.19 [a]
Control [γ]	0	0	0

[α]All data are averages (± SEM) from ten independent plants.. Acetylene reduction activity of nodules induced by *fmoA* mutant strain HKfmoA or complementary strain HKfmoA(pBBRfmoA) was compared to that of nodules induced by the wild-type strain 7653R.

[β a,b] Values in each column followed by the same letter are not significantly different ($P \leq 0.05$).

[γ] Control: without inoculation.

Expression level of the *fmoA* gene in 7653R-inoculated nodules

Expression of the *fmoA* gene in root nodules collected at 14 days, 28 days and 42 days post inoculation was detected by qRT-PCR (Fig. 4). The *fmoA* gene expression is significantly up-regulated in the early stage of nodule formation (14 d), the nodule maturation stage (28 d) and the late stage (42 d) of nodule development and senescence, and the *fmoA* gene has the highest expression level (more than 7-fold) in nodules at 14 days post inoculation. Therefor, *fmoA* gene expression was induced during the symbiotic interaction when compared with free-living cells growing in synthetic medium. and FmoA may play an important role in persistence of nodule bacteroids and prevention of premature nodule senescence.

RNA-seq analyses of gene expression in the nodule bacteroids

To investigate the global effects of FmoA on the gene transcription pattern of *M. huakuii* in the nodules of *A. sinicus*, the root nodules infected with a *M. huakuii* wild-type or an *fmoA* gene mutant strain were processed at 28 dpi and analyzed by transcriptomics. cDNA samples from the nodule formed by *M. huakuii* HKfmoA and 7653R were sequenced using Illumina paired-end sequencing. A total of 53-million clean sequencing reads was obtained from the RNA-seq transcriptomics analysis of two samples, with average reads of 26.5-million reads per sample. In total, 6721 expressed genes were detected in both the *M. huakuii* strains during symbiosis through RNA-SEq. Comparative analysis of gene expression levels found that 1233 genes were differentially expressed (p-value ≤ 0.01, with $\log_2$ (FC) ≥ 1.5 and ≤ -1.5), of which 560 were up-regulated and 673 were down-regulated in *M. huakuii* HKfmoA bacteroids compared to in *M. huakuii* 7653R bacteroids. Among these differentially expressed genes, 1164 (94.4%) were located on the chromosome, 32 (2.6%) were located on the plasmid pMHa, and 37 (3.0%) were located on the symbiotic plasmid pMHb. Symbiotic genes such as *nif*, *fix* and *nod* genes, are located on symbiotic plasmid pMHb. However, there was no difference in expression levels of these genes between *fmoA* mutant bacteroids and wild-type 7653R bacteroids.

To categorize these differences into modules of biological relevance, the top 500 differential expression genes (FC > 2, p < 0.005) were annotated by Clusters of Orthologous Groups (COG) (Table S1). They were functionally classified into 19 categories, which mainly were involved in amino acid transport and metabolism (n = 61, 12.2%), transcription (n = 49, 9.8%), cell wall/membrane/envelope biogenesis (n = 47, 9.4%), carbohydrate transport and metabolism (n = 46, 9.2%), posttranslational modification, protein turnover, chaperones (n = 35, 7.0%), inorganic ion transport and metabolism (n = 33, 6.6%), but the percentages of cell cycle control, cell division, chromosome partitioning, and nucleotide transport and metabolism, and defense mechanisms, and intracellular trafficking, secretion, and vesicular transport, and signal transduction mechanisms, were < 3.00%. None of the genes were assigned to RNA processing and modification, chromatin structure and dynamics, secondary metabolites biosynthesis, transport and catabolism, extracellular structures, and cytoskeleton (Fig. 5).

Among the top 500 regulated genes, 242 were up-regulated in nodules induced by the *fmoA* mutant. All the cell motility genes were found to be significantly up-expressed (Fig. 5), the category includes the cell motility flagella structural genes (*fliIKLMPQ* and *flgABCDEFGHI*), a flagellar biosynthesis repressor gene (*flbT*), a flagellar motor stator protein gene *motA* and a chemotaxis protein gene *motC* (*MCHK_4458*) (Table 4). And the two categories “carbohydrate transport and metabolism”, and “coenzyme transport and metabolism” were also found to be significantly over-represented among these genes (Fig. 5). 35 carbohydrate transport and metabolism genes were found among the top 500 genes showing increased expression in mutant nodules: ten coding for ABC transporters; three coding for tripartite tricarboxylate transporters. The coenzyme transport and metabolism were up-regulated including five biotin mechanism genes, four cobalt mechanism genes, two nicotinate-nucleotide genes, and a thiamine biosynthesis gene *thiS*. Interestingly, these coenzymes all play an indispensable role in rhizobial growth or nitrogenase activity (Table 4).

Table 4
List of 81 genes that showed significantly increased expression in *A. sinicus* nodules.

Gene ID	Description	log_2(*fmoA* mt nod vs wt nod)[α]
Carbohydrate transport and metabolism		
MCHK_4670	tripartite tricarboxylate transporter permease	2.94
MCHK_4672	tripartite tricarboxylate transporter substrate binding protein	2.41
MCHK_5078	D-xylose ABC transporter substrate-binding protein	3.58
MCHK_5077	sugar ABC transporter permease	3.53
MCHK_1803	ribokinase	3.31
MCHK_7127	GHMP kinase	3.29
MCHK_5076	sugar ABC transporter ATP-binding protein	3.21
MCHK_4751	sugar phosphate isomerase/epimerase	3.16
MCHK_6220	C4-dicarboxylate ABC transporter	3.12
MCHK_3455	ABC transporter permease	3.03
MCHK_5818	2-dehydro-3-deoxy-6-phosphogalactonate aldolase	2.97
MCHK_1547	ABC transporter substrate-binding protein	2.88
MCHK_3280	ABC transporter permease	2.81
MCHK_8253	transketolase	2.81
MCHK_1755	sugar ABC transporter substrate-binding protein	2.73
MCHK_6219	iditol 2-dehydrogenase	2.68
MCHK_1863	inositol monophosphatase	2.63
MCHK_6099	xylose isomerase	2.62
MCHK_4690	ribokinase	2.40
MCHK_5166	pyruvate kinase	2.38
MCHK_5079	ROK family protein	2.38
MCHK_1054	alpha-D-glucose phosphate-specific phosphoglucomutase	2.36

[α] log_2 of the fold change (FC) in expression of *A. sinicus* nodules induced by an FmoA mutant (*fmoA* mt nod) versus the wild type 7653R (wt nod); GHMP kinase: the galactokinase, homoserine kinase, mevalonate kinase, and phosphomevalonate kinase; ROK: repressor, open reading frame, kinase; MFS: major facilitator superfamily.

Gene ID	Description	log_2(*fmoA* mt nod vs wt nod)[α]
MCHK_0860	chloromuconate cycloisomerase	2.34
MCHK_6260	3-phosphoshikimate 1-carboxyvinyltransferase	2.34
MCHK_0198	6-phosphogluconolactonase	2.32
MCHK_0749	D-allulose-6-phosphate 3-epimerase	2.29
MCHK_4514	keto-deoxy-phosphogluconate aldolase	2.25
MCHK_1055	glycogen debranching enzyme GlgX	2.24
MCHK_4577	alcohol dehydrogenase	2.23
MCHK_3233	ABC transporter permease	2.22
MCHK_4335	MFS transporter	2.27
MCHK_1904	histone deacetylase family protein	2.65
MCHK_0856	ABC transporter ATP-binding protein	2.17
MCHK_1905	N-acetyltransferase	2.48
MCHK_4671	tripartite tricarboxylate transporter TctB family protein	2.32
Coenzyme transport and metabolism		
MCHK_7220	8-amino-7-oxononanoate synthase	4.01
MCHK_7221	ATP-dependent dethiobiotin synthetase BioD	3.91
MCHK_2994	nicotinate-nucleotide–dimethylbenzimidazole phosphoribosyltransferase	3.58
MCHK_2992	cobyrinate a%2Cc-diamide synthase	3.34
MCHK_7217	nicotinate-nucleotide diphosphorylase (carboxylating)	3.16
MCHK_2985	precorrin-2 C(20)-methyltransferase	3.12
MCHK_2984	precorrin-8X methylmutase	2.95
MCHK_7214	quinolinate synthase NadA	2.91
MCHK_2991	uroporphyrinogen-III C-methyltransferase	2.80
MCHK_3795	thiamine biosynthesis protein ThiS	2.68

[α] log_2 of the fold change (FC) in expression of *A. sinicus* nodules induced by an FmoA mutant (*fmoA* mt nod) versus the wild type 7653R (wt nod); GHMP kinase: the galactokinase, homoserine kinase, mevalonate kinase, and phosphomevalonate kinase; ROK: repressor, open reading frame, kinase; MFS: major facilitator superfamily.

Gene ID	Description	log_2(*fmoA* mt nod vs wt nod)[α]
MCHK_2986	precorrin-3B C(17)-methyltransferase	2.59
MCHK_2981	cobalamin biosynthesis protein CobW	2.56
MCHK_7219	biotin synthase BioB	2.40
MCHK_2963	biotin–[acetyl-CoA-carboxylase] ligase	2.38
MCHK_1992	acetyl-CoA carboxylase biotin carboxyl carrier protein	2.31
MCHK_2928	cob(I)yrinic acid a%2Cc-diamide adenosyltransferase	2.30
MCHK_0194	bifunctional methylenetetrahydrofolate dehydrogenase/methenyltetrahydrofolate cyclohydrolase FolD	2.28
MCHK_2982	cobaltochelatase subunit CobN	2.21
MCHK_3415	FAD-binding oxidoreductase	2.69
MCHK_3053	FAD-dependent monooxygenase	2.27
Cell motility		
MCHK_4462	flagellar hook protein FlgE	4.83
MCHK_4441	flagellar biosynthesis protein FlgB	4.22
MCHK_4463	flagellar hook-associated protein FlgK	4.21
MCHK_4444	flagellar basal-body rod protein FlgG	3.80
MCHK_4453	flagellin	3.76
MCHK_4442	flagellar basal body rod protein FlgC	3.60
MCHK_4446	flagellar basal body P-ring protein FlgI	3.55
MCHK_4457	flagellar motor protein MotB	3.48
MCHK_4443	flagellar hook-basal body protein FliE	3.26
MCHK_4494	flagellar biosynthesis protein FlgJ	3.24
MCHK_4448	flagellar basal body L-ring protein FlgH	3.20
MCHK_4436	flagellar motor stator protein MotA	3.18
MCHK_4464	flagellar hook-associated protein FlgL	2.95

[α] log_2 of the fold change (FC) in expression of *A. sinicus* nodules induced by an FmoA mutant (*fmoA* mt nod) versus the wild type 7653R (wt nod); GHMP kinase: the galactokinase, homoserine kinase, mevalonate kinase, and phosphomevalonate kinase; ROK: repressor, open reading frame, kinase; MFS: major facilitator superfamily.

Gene ID	Description	log_2(*fmoA* mt nod vs wt nod)[α]
MCHK_4435	flagellar motor switch protein FliM	2.79
MCHK_4439	flagellum-specific ATP synthase FliI	2.77
MCHK_4445	flagella basal body P-ring formation protein FlgA	2.73
MCHK_4450	flagellar biosynthetic protein FliP	2.68
MCHK_4468	flagellar biosynthetic protein FliQ	2.66
MCHK_4467	flagellar basal body rod modification protein FlgD	2.61
MCHK_4459	flagellar hook-length control protein FliK	2.48
MCHK_4466	flagellar biosynthesis repressor FlbT	2.45
MCHK_4449	flagellar basal body-associated protein FliL	2.37
MCHK_4483	flagellar biosynthesis protein FlhA	2.31
MCHK_4438	flagellar basal-body rod protein FlgF	2.26
MCHK_4458	chemotaxis protein MotC	2.25
MCHK_4455	flagellar M-ring protein FliF	3.36

[α] log_2 of the fold change (FC) in expression of *A. sinicus* nodules induced by an FmoA mutant (*fmoA* mt nod) versus the wild type 7653R (wt nod); GHMP kinase: the galactokinase, homoserine kinase, mevalonate kinase, and phosphomevalonate kinase; ROK: repressor, open reading frame, kinase; MFS: major facilitator superfamily.

In contrast, among the 258 genes down-regulated in *fmoA* nodule bacteroids, the four categories “transcription”, “defense mechanisms”, “signal transduction mechanisms”, and “posttranslational modification, protein turnover, chaperones” were notably over-represented (Fig. 5). All the defense mechanism genes were found to be significantly down-expressed. The defense mechanism category includes seven genes encoding stress response and virulence proteins (Table 5). And the category “posttranslational modification, protein turnover, chaperones” also includes stress response genes encoding heat-shock proteins and antioxidant proteins (Table 5). The signal transduction mechanism category includes two histidine kinases, a sensory box protein, a circadian clock protein KaiC and a phage-shock protein (Table 5). Moreover, 42 transcription regulators were found among the top 500 genes showing reduced expression in mutant nodules: *MCHK_1343*, *MCHK_4626*, and *MCHK_5064* coding for the cyclic AMP receptor protein (Crp)- fumarate and nitrate reduction regulator (FNR) family transcriptional regulators; *MCHK_4665* and *MCHK_2899* coding for the AraC family transcriptional regulators; *MCHK_5909* coding for Lrp/AsnC family transcriptional regulator; *MCHK_2407* coding for a DeoR/GlpR-type protein; *MCHK_4182* coding for a PadR family transcriptional regulator; *MCHK_1555* coding for a MarR family transcriptional regulator; *MCHK_5264* coding for a ArsR family transcriptional

regulator; *MCHK_5463* coding for transcriptional regulator GcvA; six TetR/AcrR family transcriptional regulators; and two LysR family transcriptional regulators (Table 5).

Table 5
List of 81 genes that showed significantly decreased expression in *A. sinicus* nodules.

Gene ID	Description	log_2(*fmoA* mt nod vs wt nod)[α]
Transcription		
MCHK_2899	AraC family transcriptional regulator	-2.58
MCHK_5264	ArsR family transcriptional regulator	-2.84
MCHK_5596	ArsR family transcriptional regulator	-3.31
MCHK_4665	bacterial regulatory helix-turn-helix s, AraC family protein	-3.24
MCHK_1343	Crp/Fnr family transcriptional regulator	-2.17
MCHK_4626	Crp/Fnr family transcriptional regulator	-3.07
MCHK_5064	Crp/Fnr family transcriptional regulator	-4.14
MCHK_2407	DeoR/GlpR transcriptional regulator	-2.38
MCHK_6151	DNA-binding response regulator	-2.44
MCHK_5293	HxlR family transcriptional regulator	-2.26
MCHK_6070	LacI family transcriptional regulator	-2.39
MCHK_5909	Lrp/AsnC family transcriptional regulator	-2.32
MCHK_5172	LysR family transcriptional regulator	-2.43
MCHK_8319	LysR family transcriptional regulator	-2.51
MCHK_1555	MarR family transcriptional regulator	-2.51
MCHK_6203	MarR family transcriptional regulator	-3.67
MCHK_2346	nuclear transport factor 2 family protein	-2.41
MCHK_4182	PadR family transcriptional regulator	-2.48
MCHK_3131	response regulator	-4.55
MCHK_3765	response regulator	-2.60
MCHK_5675	Rrf2 family transcriptional regulator	-2.19

[α] log_2 of the fold change (FC) in expression of *A. sinicus* nodules induced by an FmoA mutant (*fmoA* mt nod) versus the wild type 7653R (wt nod); CRP: cyclic AMP receptor protein; FNR: fumarate and nitrate reduction regulator; DeoR: double extended octagonal ring; GlpR: the glycerol-phosphate regulon repressor; Lrp/AsnC: leucine-responsive regulatory protein/asparagine synthase C products; TetR: the tetracycline repressor; AcrR: Acriflavine resistance regulator;

Gene ID	Description	log_2(*fmoA* mt nod vs wt nod)[α]
MCHK_6404	Rrf2 family transcriptional regulator	-2.38
MCHK_0869	TetR/AcrR family transcriptional regulator	-2.59
MCHK_1530	TetR/AcrR family transcriptional regulator	-2.72
MCHK_4596	TetR/AcrR family transcriptional regulator	-2.81
MCHK_4079	TetR/AcrR family transcriptional regulator	-2.89
MCHK_5377	TetR/AcrR family transcriptional regulator	-3.22
MCHK_5899	TetR/AcrR family transcriptional regulator	-4.38
MCHK_1081	transcriptional regulator BetI	-3.05
MCHK_5463	transcriptional regulator GcvA	-2.84
MCHK_4196	transcriptional regulator	-2.30
MCHK_3666	transcriptional regulator	-2.48
MCHK_4190	transcriptional regulator	-2.94
MCHK_7254	transcriptional regulator	-2.95
MCHK_8309	transcriptional regulator	-3.16
MCHK_4740	transcriptional repressor	-2.47
MCHK_5069	two-component response regulator	-3.54
MCHK_8032	XRE family transcriptional regulator	-2.82
MCHK_1392	XRE family transcriptional regulator	-4.49
Posttranslational modification, protein turnover, chaperones		
MCHK_5347	aldo/keto reductase	-2.91
MCHK_5345	aldo/keto reductase	-3.06
MCHK_2360	ATP-dependent Clp protease adapter ClpS	-2.99
MCHK_4308	ATP-dependent Clp protease adapter protein ClpS 2	-2.62
MCHK_6078	ATP-dependent protease subunit HslV	-2.76

[α] log_2 of the fold change (FC) in expression of *A. sinicus* nodules induced by an FmoA mutant (*fmoA* mt nod) versus the wild type 7653R (wt nod); CRP: cyclic AMP receptor protein; FNR: fumarate and nitrate reduction regulator; DeoR: double extended octagonal ring; GlpR: the glycerol-phosphate regulon repressor; Lrp/AsnC: leucine-responsive regulatory protein/asparagine synthase C products; TetR: the tetracycline repressor; AcrR: Acriflavine resistance regulator;

Gene ID	Description	log_2(*fmoA* mt nod vs wt nod)[a]
MCHK_5613	ATP-dependent protease	-2.21
MCHK_4683	class I SAM-dependent methyltransferase	-3.52
MCHK_1111	cysteine desulfuration protein SufE	-2.16
MCHK_2694	cytochrome c oxidase subunit I	-3.72
MCHK_1836	Fe-S cluster assembly protein SufB	-2.37
MCHK_4860	glutaredoxin 3	-3.09
MCHK_4360	glutathione S-transferase family protein	-3.26
MCHK_3585	glutathione-dependent disulfide-bond oxidoreductase	-3.06
MCHK_4694	heat-shock protein Hsp20	-3.57
MCHK_4545	heat-shock protein IbpA	-5.24
MCHK_3507	heat-shock protein	-5.82
MCHK_2737	iron-sulfur cluster assembly accessory protein	-2.95
MCHK_2657	iron-sulfur cluster assembly scaffold protein	-2.43
MCHK_2576	isoprenylcysteine carboxylmethyltransferase family protein	-2.39
MCHK_4078	macrocin O-methyltransferase	-2.28
MCHK_3347	peptide-methionine (S)-S-oxide reductase	-4.04
MCHK_7135	peroxiredoxin	-4.37
MCHK_0445	plasmid stabilization system protein	-4.35
MCHK_5206	post-segregation antitoxin CcdA	-2.48
MCHK_6140	thioredoxin	-2.40
MCHK_5358	transglutaminase family protein	-4.45
MCHK_0971	transglutaminase	-2.35
MCHK_5361	zinc metalloprotease HtpX	-3.01

[a] log_2 of the fold change (FC) in expression of *A. sinicus* nodules induced by an FmoA mutant (*fmoA* mt nod) versus the wild type 7653R (wt nod); CRP: cyclic AMP receptor protein; FNR: fumarate and nitrate reduction regulator; DeoR: double extended octagonal ring; GlpR: the glycerol-phosphate regulon repressor; Lrp/AsnC: leucine-responsive regulatory protein/asparagine synthase C products; TetR: the tetracycline repressor; AcrR: Acriflavine resistance regulator;

Gene ID	Description	log_2(*fmoA* mt nod vs wt nod)[α]
MCHK_5608	Zn-dependent protease	-2.82
Signal transduction mechanisms		
MCHK_3972	circadian clock protein KaiC	-2.50
MCHK_8036	EF-hand domain-containing protein	-2.59
MCHK_5071	histidine kinase	-3.55
MCHK_3130	histidine kinase	-4.74
MCHK_4080	phage-shock protein	-7.43
MCHK_3762	sensory box protein	-3.14
Defense mechanisms		
MCHK_4226	addiction module antidote protein%2C HigA family	-3.56
MCHK_5059	multidrug transporter	-2.80
MCHK_5207	plasmid maintenance protein CcdB	-2.51
MCHK_3336	pyridoxamine 5'-phosphate oxidase family protein	-4.33
MCHK_5751	RidA family protein	-3.22
MCHK_5230	type II toxin-antitoxin system ParD family antitoxin	-2.74
MCHK_4136	YihY/virulence factor BrkB family protein	-3.28

[α] log_2 of the fold change (FC) in expression of *A. sinicus* nodules induced by an FmoA mutant (*fmoA* mt nod) versus the wild type 7653R (wt nod); CRP: cyclic AMP receptor protein; FNR: fumarate and nitrate reduction regulator; DeoR: double extended octagonal ring; GlpR: the glycerol-phosphate regulon repressor; Lrp/AsnC: leucine-responsive regulatory protein/asparagine synthase C products; TetR: the tetracycline repressor; AcrR: Acriflavine resistance regulator;

Discussion

Flavin-containing monooxygenase (FMO), which can metabolize numerous foreign chemicals, is a monooxygenase that uses the reducing equivalents of NADPH to reduce one atom of molecular oxygen to water, while the other atom is used to oxidize the substrate [21]. An important issue is that *M. huakuii fmoA* expression is elevated in nitrogen-fixing bacteroids of the *A. sinicus* root nodules, but no studies have been published regarding the connection between the legumes-root nodule bacteria nitrogen fixing system and the function of FmoA. In this study, we focus on a *fmoA* mutant strain of *M. huakuii* that is affected with regard to its symbiotic capacity and oxidative stress response.

Flavin-containing monooxygenases (FMOs) have been reported to be important for the disposition of many therapeutics, environmental toxicants, and nutrients and, thus, mediate interactions between organisms and their chemical environment [22, 23] Mutation of *fmoA* can only slightly reduce the growth rate of *M. huakuii* in AMS with D-glucose as a sole carbon source, but displayed decreased growth capacity in the presence of high concentrations of inorganic peroxide H_2O_2 and organic peroxide CUOOH (Table 1). Intracellular H_2O_2 content was measured in the mutant, showing a significantly low H_2O_2 content compared to the wild type when FmoA was not present (Table 2). No research could demonstrate that FMO functioned as the defence against the peroxides, but human FMOs as a source of hydrogen peroxide released 30–50% of O_2 consumed as H_2O_2 upon addition of NADPH [24], and liver flavin-containing monooxygenase has also been shown to exhibit a stable 4a-flavin hydroperoxide intermediate in the absence of oxygenatable substrate [25], suggesting the presence of FMO may increase cellular peroxide concentration, therefor may improve tolerance of exogenous H_2O_2. In aerobic cells, GSH is the most abundant antioxidant [26]. The effects of H_2O_2 stress on the activities of antioxidant enzymes such as peroxidase and glutathione reductase, and the content of GSH were further investigated. The antioxidant enzyme activities of mutant HKfmoA were no difference compared to that of wild type strain 7653R, but its GSH content was significantly lower (Table 2), suggesting that *M. huakuii* FmoA-deficiency-mediated decrease in glutathione increases the sensitivity of mutant cells to peroxides.

Since *M. huakuii fmoA* gene expression is significantly up-regulated on the whole nodulation process, and it's the highest expression level occurred at 14 days after inoculation (Fig. 4). The roles of FmoA in symbiotic nitrogen fixation and the colonization of the plant rhizosphere were further studied by plant experiments. Although the expression levels of symbiotic genes such as *nif*, *fix* and *nod*, were not significantly different in bacteroids from the fmoA mutant and the wild-type strain, *A. sinicus* plants inoculated with the *fmoA* mutant exhibited a large decrease in the nitrogen-fixing activity of root nodules (reduced by more than 65%) (Table 3). Further investigation revealed that *fmoA* mutant HKfmoA-induced nodules were spherical rather than elongated, underwent premature senescence, and PHB granules could be detected in the fmoA mutant bacteroids but not in those of the wild-type strain (Fig. 3). Moreover, the *M. huakuii fmoA* mutant was unable to compete efficiently in the rhizosphere with its wild-type 7653R. Flavin-containing monooxygenases metabolize a vast array of foreign chemicals including antioxidants, phytochemicals and dietary components, and, thus, mediate interactions between bacteria and their chemical environment [19]. The results showed that bacterial FmoA was important for adaptation to the microenvironment of the plant host (Fig. 2). Overall, considering the poor nitrogen-fixing ability of its nodules, the mutant in *fmoA* gene has a profound influence on the whole nodulation process.

The RNA-seq experiments were performed to provide a foundation for assessing the influence of FmoA on the symbiotic nitrogen fixation. In this study, the carbohydrate transport and metabolism, coenzyme transport and metabolism, and flagellar genes were found to be significantly up-expressed in *fmoA* mutant induced bacteroids (Fig. 5). Flagellar motility is a critical environmental adaptation for the plant-associated bacteria such as *Rhizobium* that allows bacteria to escape adverse conditions and populate new environments [27]. The up-regulation of flagellar genes in this case might be due to the hostile

environment in which the bacteroids with low nitrogenase activity are embedded [28]. In the *fmoA* mutant-induced nodules, many symbiosomes were aberrant and the bacteroid membrane showed incrassation (Fig. 3). The peribacteroid membrane may be relatively impermeable to sugars and so dictate the carbon source(s) available to the bacteroids [29]. This might also be the reason for the over-represented up-regulation category “coenzyme transport and metabolism”. The up-expression of carbohydrate transport and metabolism category containing 10 ABC transporter genes might be due to a delicate balance control between sufficient acquisition and overload (Table 4). In this study, PHB was occured in the *fmoA* mutant bacteroids (Fig. 4). During the formation of bacteroids in indeterminate-type nodules such as *M. huakuii*, the PHB granules are broken down. PHB can be used as a carbon and energy source for bacteroid formation, but most rhizobial species such as *M. huakuii* do not accumulate it during symbiosis with legumes. Biochemically, PHB synthesis directly competes with N_2 fixation for reductant. PHB synthesis is apparently a concomitant reduction in protein synthesis, a process coupled to ATP formation and utilization [30]. PHB granules occurred in undergoing senescence bacteroids infected by *fmoA* mutant implied that the energy and carbon metabolism was shifted, NAD(P)H was channeled into other biosynthesis reactions, such as PHB synthesis [31].

Among the the down-exprssion genes, the four categories “Transcription”, “Defense mechanisms”, “Signal transduction mechanisms”, and “Posttranslational modification, protein turnover, chaperones” were significantly over-represented (Fig. 5). One of the remarkable findings of the RNA-seq analysis was that nearly all the genes associated with stress response and virulence were significantly differentially down-expressed (Table 5). The symbiotic nodule is prone to high levels of ROS due to the high rate of respiration necessary to supply energy required for nitrogen reduction by nitrogenase [32], but increased level of ROS causes oxidative damage to important cellular macromolecules [33]. Thiol-containing molecules, such as glutathione, glutathione S-transferases, glutaredoxins, and peroxiredoxins play an important role in maintaining redox homeostasis and redox regulation [34]. Nodules induced by *fmoA* mutant bacteria presented the lower expression of the thiol-containing molecules, which was associated with increased levels of superoxide accumulation. It has been reported that heat shock proteins play important roles in innate immune responses [35], and in *Agrobacterium*, the virulence genes are essential for attachment to plant cells [36]. The expression of three heat-shock protein and several virulence genes was also decreased in the *fmoA* mutant nodules (Table 5). Therefor, the results suggested that the stress response function of *M. huakuii* is influenced by deletion of the *fmoA* gene. In addition, it has been reported that the sensor histidine kinase mediated the pathogenesis by the bacterium *Rhizobium radiobacter* [37], and mutation of a *R. leguminosarum* histidine kinase gene *chvG* destabilized the outer membrane of *R. leguminosarum*, resulting in increased sensitivity to membrane stressors, and caused symbiotic defects on peas, lentils, and vetch [38]. In early senescent nodules induced by the *fmoA* mutant, the expression of two histidine kinases and a sensory box protein was significantly decreased, suggesting that FmoA could influence the symbiotic interaction between *M. huakuii* and *A. sinicus* by decreasing the expression of sensor molecules.

Moreover, 42 transcriptional regulator genes were found among the top 500 genes showing reduced expression (Table 5). *MCHK_1343*, *MCHK_4626*, and *MCHK_5064* coding for the Crp-Fnr family transcriptional regulators, which is an important transcriptional regulator that controls the expression of a large regulon of more than 100 genes in response to changes in oxygen availability [49]; *MCHK_4665* and *MCHK_2899* coding for the AraC family transcriptional regulators, which play a critical role in regulating bacterial virulence factors in response to environmental stress [40]; *MCHK_5909* coding for Lrp/AsnC family transcriptional regulator, which is known as feast/famine regulatory protein (FFRPs) [41]; *MCHK_2407* coding for a DeoR/GlpR-type protein, which serves as transcriptional repressor or activator of either sugar or nucleoside metabolism [42, 43]; *MCHK_4182* coding for a PadR family transcriptional regulator that functioned as environmental sensor [44]; *MCHK_1555* coding for a MarR family transcriptional regulator, which is involved in the regulation of many cellular processes, including pathogenesis [45]; *MCHK_5264* coding for a ArsR family transcriptional regulator involved in symbiosis and virulence [46]; *MCHK_5463* coding for transcriptional regulator GcvA, which is required for both glycine-mediated activation and purine-mediated repression of the gcvTHP operon [47]. Taken together, nodules induced by the fmoA mutant are different from those induced by the wild-type strain, and there is also a clear difference in bacteroid aspect, revealing that the fmoA mutant is negatively affected in symbiosis. The reduced nitrogen fixation ability exhibited by the fmoA mutant could be a consequence of a defect in nodule development

Conclusions

Flavin-containing monooxygenases (FMOs) catalyze the oxidation of heteroatom centers and, thus, mediate interactions between microorganisms and their chemical environment. The contribution of FmoA to symbiosis and anti-oxidative damage was investigated using the *M. huakuii fmoA* mutant. A quantitative RNA-Seq based transcriptomics approach was applied to reveal the global transcriptomic responses to FmoA defect in *M. huakuii* bacteroids from *A. sinicus* root nodules. The results showed a total of 1233 genes were differentially expressed, of which 560 were up-regulated and 673 were down-regulated in HKfmoA bacteroids compared to that in 7653R bacteroids. This study provided majority of these differentially expressed genes were grouped into 19 categories and a valuable insight into FmoA-mediated mechanisms during *M. huakuii-A. sinicus* symbiosis. Furthermore, this study has generated an abundant list of transcript from *M. huakuii* which will provide a fundamental basis for future functional genomic research in *M. huakuii* and other closely related species.

Methods

Bacterial growth and media

The strains, plasmids and primers used in this study are listed in Table S2. *M. huakuii* strains were grown at 28 °C in either Tryptone Yeast extract (TY) [48] or Acid Minimal Salts medium (AMS) [49] with D-glucose (10 mM) as a carbon source and NH_4Cl (10 mM) as a N source. For growth and qRT-PCR (real-

time reverse transcription-PCR) experiments, cells were grown in AMS. When required, the following antibiotics were used at the following concentrations (μg mL^{-1}): Streptomycin (Str), 500; Ampicillin (Amp), 50; Kanamycin (Km), 20; Neomycin (Neo), 80, or 250 (for making *fmoA* mutant); Gentamicin (Gm), 20; Spectinomycin (Spe), 100; Tetracycline (Tc), 5. To monitor culture growth, strains were grown at 28 °C with shaking (200 rpm) in liquid media, and culture optical density at 600 nm (OD_{600}) was measured during the culture period.

Construction and complementation of *fmoA* gene mutant strain of *M. huakuii* 7653R

A single-crossover integration mutation in *fmoA* was made in 7653R. Primers fmoAUP and fmoALW were used to PCR amplify the *fmoA* region from 7653R genomic DNA, and the 620-bp internal fragment of the *fmoA* gene was cloned into the *Pst* I and *Xba* I sites of pK19mob, giving plasmid pKfmoA. Plasmid pKfmoA was transferred from *E. coli* to 7653R and recombined into the genomic *fmoA* region via single crossover to give strain HKfmoA [49]. Insertions into the *fmoA* gene of strain 7653R were confirmed by PCR using the fmoAmap primer and a pK19mob-specific primer pK19A or pK19B [50].

To complement the *fmoA* mutant, primers cfmoAF and cfmoAR were used to amplify the complete *fmoA* gene from *M. huakuii* 7653R genomic DNA. The PCR product was digested with *Kpn* I and *Xba* I and cloned into the broad-host-range vector pBBR1MCS-5, resulting in plasmid pBBRfmoA. Plasmid pBBRfmoA was mated into the mutant strain HKfmoA using the triparental mating method as previously described [50].

Mutant resistance and catalase activity in relation to oxidative stress

The logarithmic phase *M. huakuii* HKfmoA and 7653R cultures were collected and washed in sterile phosphate-buffered saline (PBS) (1X; 136 mM NaCl, 2.6 mM KCl, 8.0 mM Na_2HPO_4, 1.5 mM KH_2PO_4) as previously described [51]. Cells were treated with H_2O_2 at the concentrations of 1 mmol/L, 5 mmol/L, 10 mmol/L or CUOOH at the concentrations of 0.1 mmol/L, 1 mmol/L, 5 mmol/L for 1 h. Strains were thoroughly washed with distilled water to remove any remaining oxidants, and diluted TY plate to evaluate the bacterial survival rate. Each treatment consisted of 3 replicates.

For measurement of enzymatic activities and non-enzymatic antioxidant contents, the logarithmic phase *M. huakuii* HKfmoA and 7653R cultures were treated with 5 mM H_2O_2 for 1 h. H_2O_2-treated PBS cells were collected by centrifugation at 5000 rpm for 5 min at 4 °C. The cells suspension was bath-sonicated for 15 sec in ice-cold water. The sonicate was centrifuged at 12,000 rpm at 4 °C for 10 min. Peroxidase activity, glutathione reductase activity, hydrogen peroxide content, and GSH content were measured spectrophotometrically using the Glutathione Reductase Assay Kit, total Glutathione Peroxidase Assay Kit, total Superoxide Dismutase Assay Kit, Hydrogen Peroxide Assay Kit, and Glutathione Assay Kit (Beyotime, China).

Plant experiment and cytological study of nodules

Astragalus sinicus L. cultivar XY202 (Xinyang Company, China) was used as a host plant to test nodulation of the *M. huakuii* strains. Seeds were surface-sterilized, placed in 500 mL pots filled with sterile vermiculite containing nitrogen-free Fahraeus solution. Inoculation with *M. huakuii* stains was performed on 7-day-old seedlings. The cultivation was carried out in a controlled environment chamber with 16 h light/8 h dark period. Acetylene reduction activity was determined at 28 day postinoculation (dpi) as previously described [52]. The experiment consisted of two independent experiments, each of which had five repeats, and statistical differences were analyzed with one-way ANOVA ($P < 0.05$).

Nodules at 28 dpi were fixed for 12 h at 4 °C with 2.5% glutaraldehyde, rinsed, and post-fixed in 1.5% phosphate-buffered osmium tetroxide. Ultra-thin sections stained with lead citrate were examined using a Hitachi H-7100 transmission electron microscope [53]. Sections were cut with a microtome and stained with toluidine blue for light microscopy.

Rhizosphere colonization

Rhizosphere colonization was performed as described previously [54]. *Astragalus sinicus* seedlings were germinated and grown for 7 days as described above for Acetylene reduction activity, and inoculated with *M. huakuii* 7653R and HKfmoA in the cfu ratios 1000:0, 0:1000, 1000:1000 and 1000:10000. Shoots were cut-off after 7 days (14 days after plant), and 20 mL of sterile phosphate-buffered saline (PBS) buffer (pH 7.4) was added to the roots and vortexed for 15 min [55]. The samples were further serially diluted and plated on TY agar plates containing either streptomycin or streptomycin and neomycin, giving the total number of viable rhizosphere- and root-associated bacteria. Each treatment consisted of 10 replications, and statistical differences were analyzed with one-way ANOVA ($P < 0.05$).

RNA isolation and quantitative RT-PCR analysis

Quantitative real-time reverse transcription PCR (qRT-PCR) was used to determine the *fmoA* gene expression level, with gene-specific primers QfmoAUP and QfmoALW. The total RNA was isolated using TRIzol reagent from free-living *M. huakuii* 7653R cultivated in AMS liquid medium, or root nodules which were harvested from *A. sinicus* inoculated with strain 7653R after 28 days postinoculation. RNA were reverse transcribed into cDNA using the SuperScript II reverse transcriptase and random hexamers. Quantitative real-time PCR analysis was performed using a SYBR Premix ExTaq kit following the manufacturer's instructions on the BIO-RAD CFX96 Real-Time PCR Detection System. The 16S rRNA gene of *M. huakuii* 7653R was used as a calibrator gene, and the data were obtained and analysed as previously described [56] .

RNA-seq library preparation and sequencing using the illumina genome analyzer

At 28 days post inoculation, the nodules of plants inoculated with HKfmoA or 7653R were harvested, immediately frozen in liquid nitrogen and stored at − 80 °C. Total cellular RNA was isolated from frozen

nodule tissues using TRIzol Reagent (Invitrogen) and RNeasy Mini Kit (Qiagen). Total RNA of each nodule sample was assessed using Agilent 2100 Bioanalyzer (Agilent Technologies, Palo Alto, CA, USA), and NanoDrop (Thermo Fisher Scientific Inc). 1 μg total RNA with RNA integrity number (RIN) value above 6.5 was used for following library preparation. The rRNA was depleted from total RNA using rRNA removal Kit. The ribosomal depleted RNA was then fragmented and reverse-transcribed into cDNA with random primers. The purified double-stranded cDNA by beads was then treated with End Prep Enzyme Mix to repair both ends and add a dA-tailing in one reaction, followed by a T-A ligation to add adaptors to both ends. Next generation sequencing library preparations were constructed according to the manufacturer's protocol. The Qsep100 (Bioptic, Taiwan, China) and Qubit 3.0 Fluorometer was used to determine the quality of the libraries.

The libraries with different indices were multiplexed and sequenced on an Illumina HiSeq instrument according to manufacturer's instructions (Illumina, San Diego, CA, USA). Sequencing was carried out by Illumina paired-end configuration. The sequencing image processing and base calling were conducted following to Illumina's protocol on the HiSeq instrument. Three independent biological replicates per sample were processed and sequenced.

Data analysis

Differences between the average of gene expression for the control and experimental groups were analyzed by the Student's t-test using SPSS software, version 18 (SPSS, Inc., Chicago, IL). For the RNA-seq study, the unique reads mapping to the *M. huakuii* genome were used for a differential gene expression analysis using the DESeq2 [57]. The P-values with false discovery rate are adjusted for multiple testing. The false discovery rate P-value < 0.01 and the absolute value of $\log_2$ (FC) ≥ 1.5 and ≤ −1.5 were used to identify statistically significant changes in gene expression. For quantitative RT-PCR analysis, $p < 0.05$ was considered to be statistically significant.

Abbreviations

FMOs: Flavin-containing monooxygenases; qRT-PCR: Quantitative real-time PCR; ROS: Reactive oxygen species; H_2O_2: Hydrogen peroxide; CUOOH: Cumene hydroperoxide; GSH: Glutathione

Declarations

Consent for publication

Not applicable.

Acknowledgements

Not applicable.

Authors’ contributions

GC conceived and designed the study. HT, QZ and SL performed the experiments. GC, HT, DH, CL, and XL analyzed the results, GC, HT and QZ wrote the manuscript. All authors read and approved the final manuscript.

Funding

This study was supported by the National Natural Science Foundation of China (31772399) and the Fundamental Research Funds for the Central Universities, South-Central University for Nationalities (CZY18022).

Availability of data and materials

Raw sequence data from these RNA-seq studies can be accessed via the NCBI Sequence Read Archive, with accession number PRJNA624718.

Ethics approval and consent to participate

Not applicable.

Competing interests

The authors declare that the research was conducted in the absence of any competing interest or commercial or financial relationships that could be construed as a potential conflict of interest.

References

1. López-Baena FJ, Ruiz-Sainz JE, Rodríguez-Carvajal MA, Vinardell JM. Bacterial molecular signals in the *Sinorhizobium fredii*-soybean symbiosis. Int J Mol Sci, 2016;17:755.
2. Janczarek M, Rachwał K, Marzec A, Grządziel J, Palusińska-Szysz M. Signal molecules and cell-surface components involved in early stages of the legume–rhizobium interactions. Appl Soil Eco, 2015;85:94-113.
3. Ibáñez F, Wall L, Fabra Starting points in plant-bacteria nitrogen-fixing symbioses: intercellular invasion of the roots. J Exp Bot, 2017;68:1905-1918.
4. Bulbul N, Kaneko Y. Co-localisation of membranes and actin in growing infected cells of Glycine max root nodules. Plant Biol, 2009;11:555-560.

5. Gage DJ. Infection and invasion of roots by symbiotic, nitrogen-fixing rhizobia during nodulation of temperate legumes. Microbiol Mol Biol Rev, 2004;68:280-300.
6. Seefeldt LC, Yang ZY, Duval S, Dean DR. Nitrogenase reduction of carbon-containing compounds. Biochim Biophys Acta, 2013;1827:1102-1111.
7. Santos R, Hérouart D, Sigaud S, Touati D, Puppo. A Oxidative burst in alfalfa- *Sinorhizobium meliloti* symbiotic interaction. Mol Plant Microbe In, 2001;14:86-89.
8. Berger A, Brouquisse R, Pathak PK, Hichri I, Singh I, Bhatia S, Boscari A, Igamberdiev AU, Gupta KJ. Pathways of nitric oxide metabolism and operation of phytoglobins in legume nodules: missing links and future directions. Plant Cell Environ, 2018;41:2057-2068.
9. Fountain JC, Bajaj P, Pandey M, Nayak SN, Yang L, Kumar V, Jayale AS, Chitikineni A, Zhuang W, Scully BT, Lee RD, Kemerait RC, Varshney RK, Guo B. Oxidative stress and carbon metabolism influence *Aspergillus flavus* transcriptome composition and secondary metabolite production. Scic Rep, 2016;6:38747.
10. Ozols J. Isolation and structure of a third form of liver microsomal flavin monooxygenase. Biochemistry, 1994;33:3751-3757.
11. Iwahana S, Iida H, Yashima E, Pescitelli G, Bari LD, Petrovic AG, Berova N. Absolute stereochemistry of a 4 a-hydroxyriboflavin analogue of the key intermediate of the fad-monooxygenase cycle. Chemistry, 2014;20:4386-4395.
12. Montellano PROD, Komives EA. Branchpoint for heme alkylation and metabolite formation in the oxidation of arylacetylenes by cytochrome p-450. J Biol Chem, 1985;260:3330-3336.
13. van Berkel WJH, Kamerbeek NM, Fraaije MW. Flavoprotein monooxygenases, a diverse class of oxidative biocatalysts. J Biotechnol, 2006;124:670-689.
14. Fraaije MW, Kamerbeek NM, van Berkel WJH, Janssen DB. Identification of a Baeyer-Villiger monooxygenase sequence motif. FEBS Lett, 2002;518:43-47.
15. Riebel A, Fink MJ, Mihovilovic MD, Fraaije MW. Type II flavin-containing monooxygenases: a new class of biocatalysts that harbors baeyer-villiger monooxygenases with a relaxed coenzyme specificity. ChemCatChem, 2014;6:1112-1117.
16. Ziegler DM. An overview of the mechanism, substrate specificities, and structure of FMOs. Drug Metab Rev, 2002;34:503–511.
17. Mayatepek E, Flock B, Zschocke J. Benzydamine metabolism in vivo is impaired in patients with deficiency of flavin-containing monooxygenase 3. Pharmacogenetics, 2004;14:775-777.
18. Chen Y, Patel NA, Crombie A, Murrell JHSC. Bacterial flavin-containing monooxygenase is trimethylamine monooxygenase. Proc Natl Acad Sci U S A, 2011;108:17791-17796.
19. Mishina TE, Zeier J. The Arabidopsis flavin-dependent monooxygenase FMO1 is an essential component of biologically induced systemic acquired resistance. Plant Physiol, 2006;141:1666-1675.
20. Suh JK, Poulsen LL, Ziegler DM, Robertus JD. Redox regulation of yeast flavin-containing monooxygenase. Arch Biochem Biophys, 2000;381:317-322.

21. Hao D, Xiao P. Prediction of sites under adaptive evolution in flavin-containing monooxygenases: selection pattern revisited. Chinese Sci Bull, 2011;56:78-92.
22. Koukouritaki SB, Poch MT, Henderson MC, Siddens LK, Krueger SK, VanDyke JE, Williams DE, Pajewski NM, Wang T, Hines RN. Identification and functional analysis of common human flavin-containing monooxygenase 3 genetic variants. J Pharmacol Exp Ther, 2007;320:266-273.
23. Phillips IR, Shephard EA. Flavin-containing monooxygenases: mutations, disease and drug response. Trends Pharmacol Sci, 2008;29:294-301.
24. Siddens LK, Krueger SK, Henderson MC, Williams DE. Mammalian flavin-containing monooxygenase (FMO) as a source of hydrogen peroxide. Biochem Pharmacol, 2014; 89:141-147.
25. Jones KC, Ballou DP. Reactions of the 4a-hydroperoxide of liver microsomal flavin containing mono-oxygenase with nucleophilic and electrophilic substrates. J Biol Chem, 1986;261:2553-2559.
26. Owen, JB, Butterfield, DA Measurement of oxidized/reduced glutathione ratio Methods Mol Biol 2010, 648, 269-277
27. Tambalo DD, Del Bel KL, Bustard DE, Greenwood PR, Steedman AE, Hynes MF. Regulation of flagellar, motility and chemotaxis genes in *Rhizobium leguminosarum* by the VisN/R-Rem cascade. Microbiology, 2010;156: 1673-1685.
28. Lardi M, Liu Y, Giudice G, Ahrens CH, Zamboni N, Pessi G. Metabolomics and transcriptomics identify multiple downstream targets of *Paraburkholderia phymatum* σ54 during symbiosis with *Phaseolus vulgaris.* Int J Mol Sci, 2018;19: 1049.
29. Saroso S, Dilworth MJ, Glenn AR. The use of activities of carbon catabolic enzymes as a probe for the carbon nutrition of snakebean nodule bacteroids. Microbiology, 1986;132:243-249.
30. Tal S, Smirnoff P, Okon Y. Purification and characterization of D-(2)-b-hydroxybutyrate dehydrogenase from *Azospirillum brasilense* Cd. J Gen Microbiol, 1990;136:645–649.
31. Xie F, Cheng G, Xu H, Wang Z, Lei L, Li Y. Identification of a novel gene for biosynthesis of a bacteroid-specific electron carrier menaquinone. PLoS One, 2011; 6:e28995.
32. Harrison J, Jamet A, Muglia CI, Van de G, Aguilar OM, Puppo A, Frendo P. Glutathione plays a fundamental role in growth and symbiotic capacity of *Sinorhizobium meliloti.* J Bacteriol, 2005;187:168-174.
33. Cobbaut M, Van Lint J. Function and regulation of protein kinase D in oxidative stress: a tale of isoforms. Oxid Med Cell Longev, 2018;2018:2138502.
34. Oktyabrsky ON, Smirnova GV. Redox regulation of cellular functions. Biochemistry, 2007;72:132-145.
35. Lo W, Liu K, Liao I, Song Y. Cloning and molecular characterization of heat shock cognate 70 from tiger shrimp (Penaeus monodon). Cell Stress Chaperon, 2004;9:332-343.
36. Dylan T, Ielpi L, Stanfield S, Kashyap L, Douglas C, Yanofsky M, Nester E, Helinski DR, Ditta G. Rhizobium meliloti genes required for nodule development are related to chromosomal virulence genes in Agrobacterium tumefaciens. Proc Natl Acad Sci U S A, 1986;83:4403-4407.

37. Fang F, Lin YH, Pierce BD, Lynn DG. A Rhizobium radiobacter histidine kinase can employ both boolean AND and OR logic gates to initiate pathogenesis. Chem Biol Chem, 2015;16:2183-2190.
38. Vanderlinde EM; Yost CK. Mutation of the sensor kinase chvg in Rhizobium leguminosarum negatively impacts cellular metabolism, outer membrane stability, and symbiosis. J Bacteriol, 2012;194:768-777.
39. Crack JC, Brun NEL, Thomson AJ, Green J, Jervis AJ. Reactions of nitric oxide and oxygen with the regulator of fumarate and nitrate reduction, a global transcriptional regulator, during anaerobic growth of *Escherichia coli.* Methods Enzymol, 2008;437:191-209.
40. Lim BS, Chong CE, Zamrod Z, Nathan S, Mohamed R. Genome-wide prediction and annotation of *Burkholderia pseudomallei* Arac/Xyls family transcription regulator. In silico biol, 2007:7:389-397.
41. Deng W, Wang H, Xie J. Regulatory and pathogenesis roles of *Mycobacterium* Lrp/Asnc family transcriptional factors. J Cell Biochem, 2011;112:2655-2662.
42. Haghjoo E, Galán JE. Identification of a transcriptional regulator that controls intracellular gene expression in *Salmonella typhi.* Mol Microbiol, 2007;64: 1549-1561.
43. Gaurivaud P, Laigret F, Garnier M, Bové JM. Characterization of FruR as a putative activator of the fructose operon of Spiroplasma citri. FEMS Microbiol Lett, 2001;19:873-878.
44. Park SC, Kwak YM, Song WS, Hong M, Yoon SI. Structural basis of effector and operator recognition by the phenolic acid-responsive transcriptional regulator PadR. Nucleic Acids Res, 2017;45:13080-13093.
45. Wei K, Tang DJ, He YQ, Feng JX, Jiang BL, Lu GT, Chen B, Tang J HpaR, a putative marr family transcriptional regulator, is positively controlled by hrpg and hrpx and involved in the pathogenesis, hypersensitive response, and extracellular protease production of *Xanthomonas campestris* pathovar *campestris.* J Bacteriol, 2007;189:2055-2062.
46. Sai R, Li Q, Xie L, Xie J. Molecular mechanisms underlying the function diversity of ArsR family metalloregulator. Crit Rev Eukaryot Gene Expr, 2017; 27:19-35.
47. Jourdan AD, Stauffer GV. Mutational analysis of the transcriptional regulator GcvA: amino acids important for activation, repression, and dna binding. J Bacteriol, 1998;180: 4865-4871.
48. Beringer JE, Hopwood DA. Chromosomal recombination and mapping in *Rhizobium leguminosarum.* Nature, 1976;264:291-293.
49. Poole PS, Blyth A, Reid CJ, Walters K. myo-Inositol catabolism and catabolite regulation in *Rhizobium leguminosarum* bv. *Viciae*. Microbiology, 1994;140: 2787-2795.
50. Karunakaran R, Haag AF, East AK, Ramachandran VK, Prell J, James EK, Scocchi M, Ferguson GP, Poole PS. BacA is essential for bacteroid development in nodules of galegoid, but not phaseoloid, legumes. J Bacteriol, 2010;192: 2920-2928.
51. Wang S, Lu T, Xue Q, Xu K, Cheng G. Antioxidation and symbiotic nitrogen fixation function of *prxA* gene in *Mesorhizobium huakuii.* MicrobiologyOpen, 2019;8:e889.

52. Allaway D, Lodwig EM, Crompton LA, Wood M, Parsons R, Wheeler TR, Poole PS. Identification of alanine dehydrogenase and its role in mixed secretion of ammonium and alanine by pea bacteroids. Mol Microbiol, 2010;36:508-515.
53. Yan H, Xiao G, Zhang J, Hu Y, Yuan F, Cole DK, Zheng C, Gao GF. SARS coronavirus induces apoptosis in Vero E6 cells. J Med Virol, 2004;73:323-331.
54. Cheng G, Karunakaran R, East AK, Munoz-Azcarate O, Poole PS. Glutathione affects the transport activity of *Rhizobium leguminosarum* 3841 and is essential for efficient nodulation. FEMS Microbiol Lett, 2017;364:fnx045.
55. *Karunakaran, R, Ebert, K, Harvey, S, Leonard, ME, Ramachandran, V, Poole, PS Thiamine is synthesized by a salvage pathway in Rhizobium leguminosarum bv Viciae strain 3841 J Bacteriol 2006, 188, 6661-6668*
56. Prell J, Bourdès A, Karunakaran R, Lopez-Gomez M, Poole PS. Pathway of Gamma-Aminobutyrate (GABA) metabolism in *Rhizobium leguminosarum* 3841 and its role in symbiosis. J Bacteriol, 2009;191:2177-2186.
57. Anders S, Huber W. Differential expression analysis for sequence count data. Genome Biol, 2010;11:R106.
58. Cheng GJ, Li YG, Zhou JC. Cloning and identification of *opa22*, a new gene involved in nodule formation by *Mesorhizobium huakuii.* FEMS Microbiol Lett, 2006;257:152-157.
59. Schäfer A, Tauch A, Jäger W, Kalinowski J, Thierbach G, Pühler A. Small mobilizable multi-purpose cloning vectors derived from the *Escherichia coli* plasmids pK18 and pK19: selection of defined deletions in the chromosome of *Corynebacterium glutamicum.* Gene, 1994;145:69-73.
60. Figurski DH, Helinski DR. Replication of an origin-containing derivative of plasmid Rk2 dependent on a plasmid function provided in trans. Proc Natl Acad Sci U S A, 1979;76:1648-1652.
61. Kovach ME, Phillips RW, Elzer PH, Roop RM, Peterson KM. pBBR1MCS: a broad-host-range cloning vector Biotechniques. 1994;16:800-802.

Figures

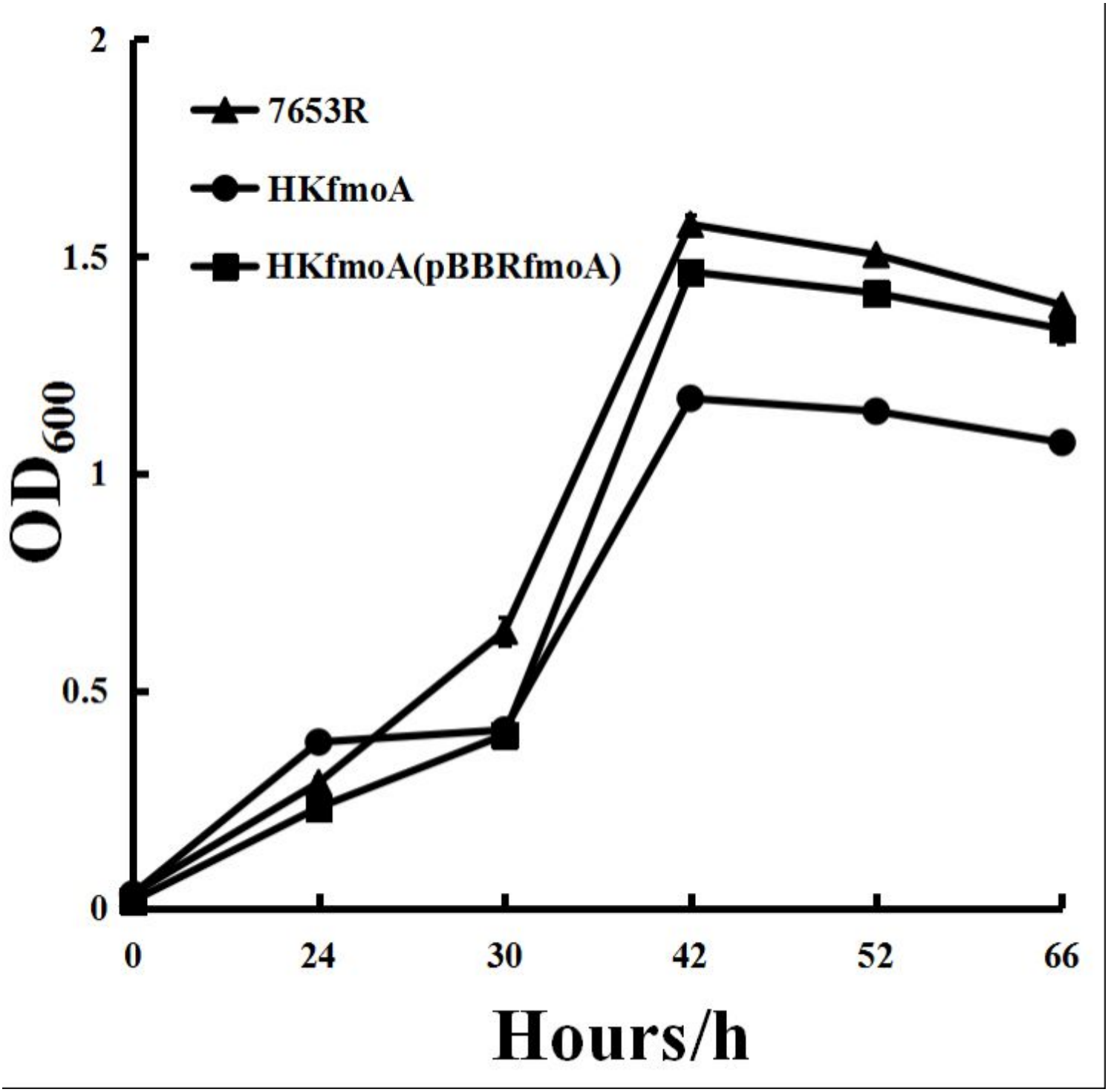

Figure 1

Growth of 7653R, fmoA mutant HKfmoA and complemented strain in AMS medium. Averages with standard errors from three independent experiments are shown.

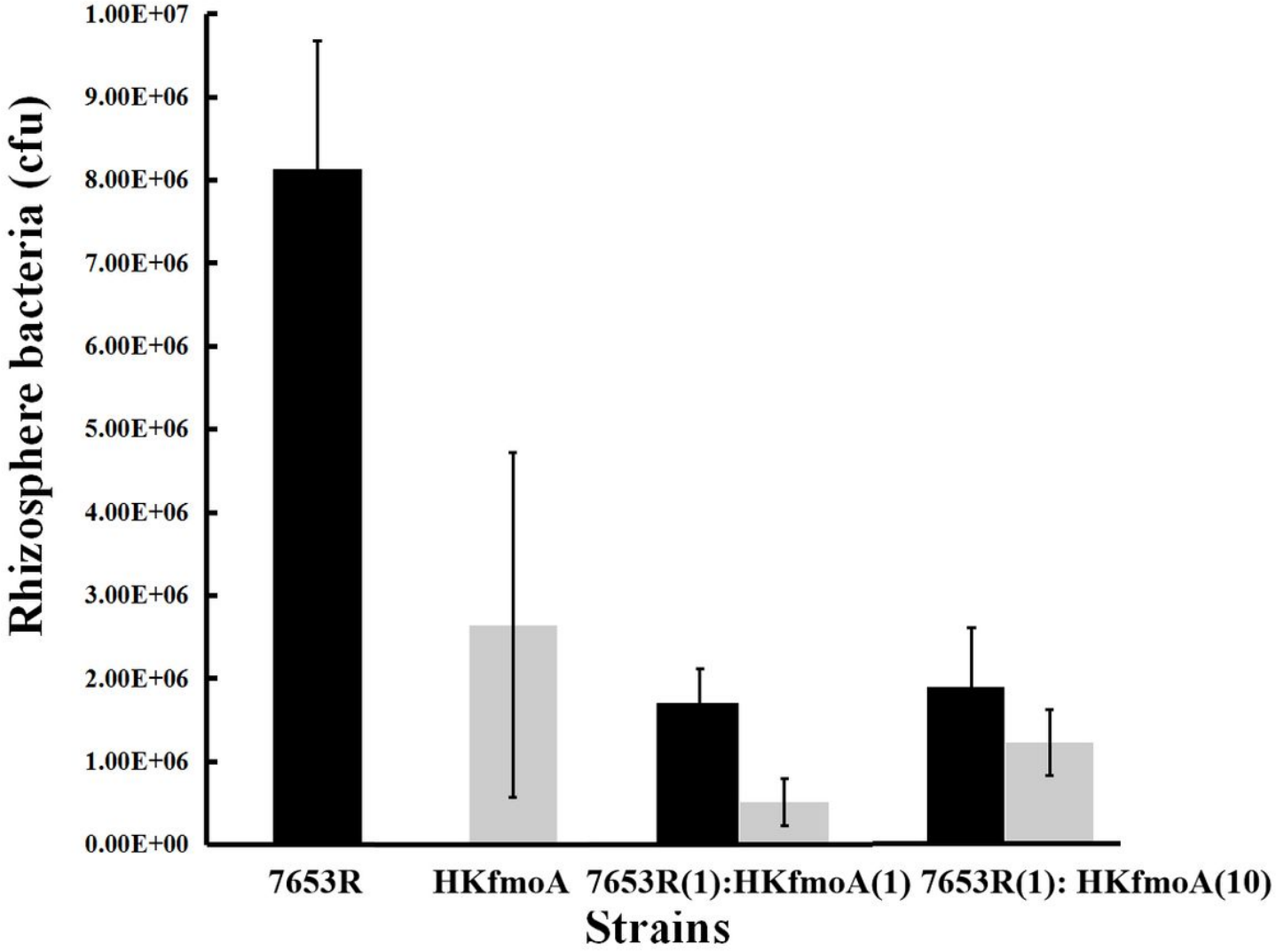

Figure 2

Bacteria recovered (7 dpi) from the rhizosphere of Astragalus sinicus plants following inoculation with wild-type 7653R and HKfmoA, both individually and together. Inoculation ratios are given on the x axis, with 1 corresponding to 103 CFU. Number of bacteria (per plant) recovered from at least ten independent plants (mean ± SEM) are shown.

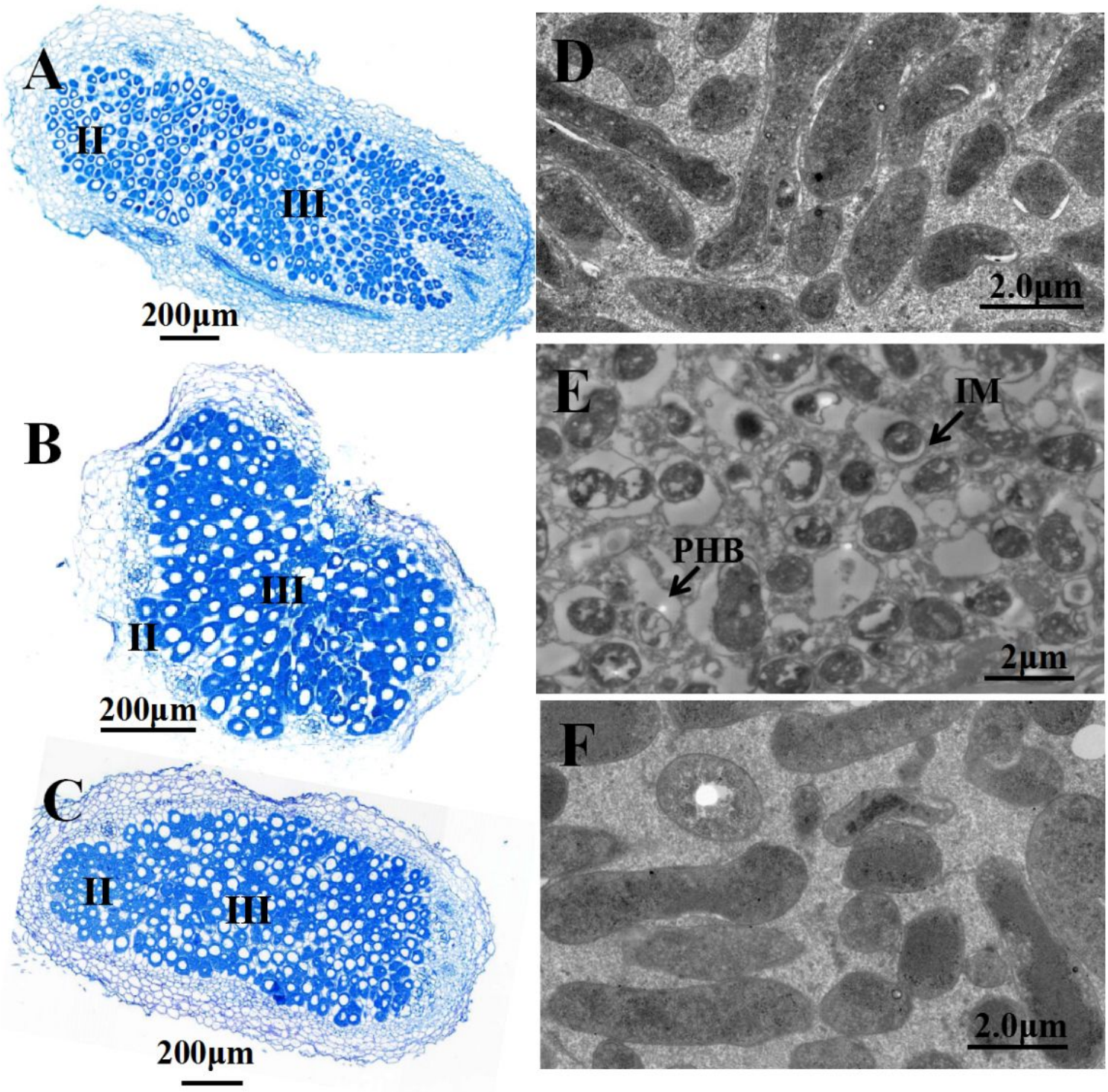

Figure 3

Structure of 4-week-old Astragalus sinicus nodules and bacteroids. Nodules were induced by M. huakuii7653R (A, D), HKfmoA (B, E), HKfmoA(pBBRfmoA) (C, F). The infection (II) and fixing (III) zones are represented in A, B and C. Scale bars = 200 μm (A, B, C), 2 μm (D, E, F). PHB, poly-β-hydroxybutyrate ; IM, incrassated membrane.

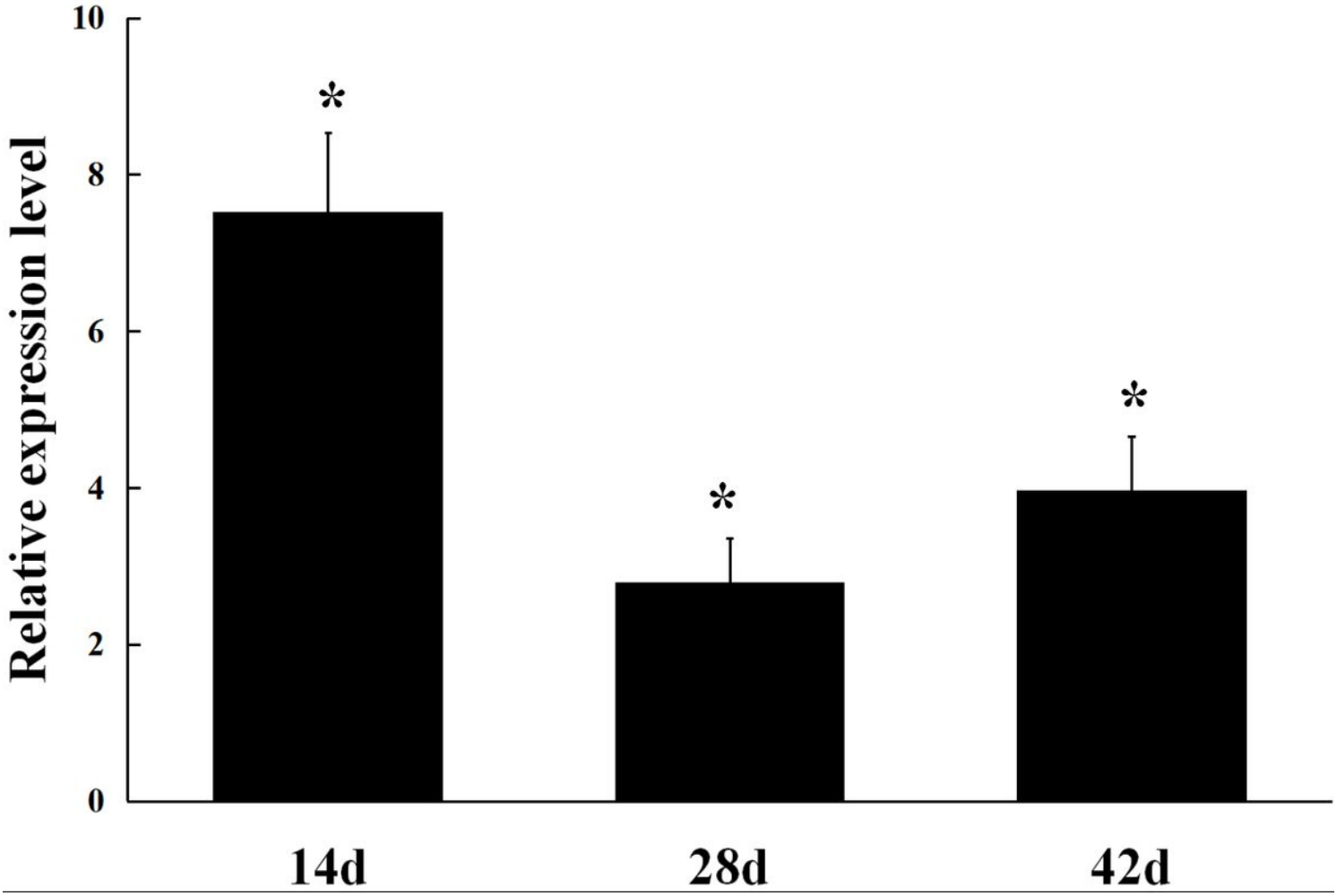

Figure 4

Expression patterns of fmoA gene in symbiotic nodules. Gene expression levels were examined by real-time RT-PCR. Nodules were collected on different days after inoculation with M. huakuii 7653R. Relative expression of genes involved in nodule bacteroids compared with 7653R cells growth in AMS medium. Data are the average of three independent biological samples (each with three technical replicates). Asterisk (*) indicates a significant difference (FC>2, P<0.05).

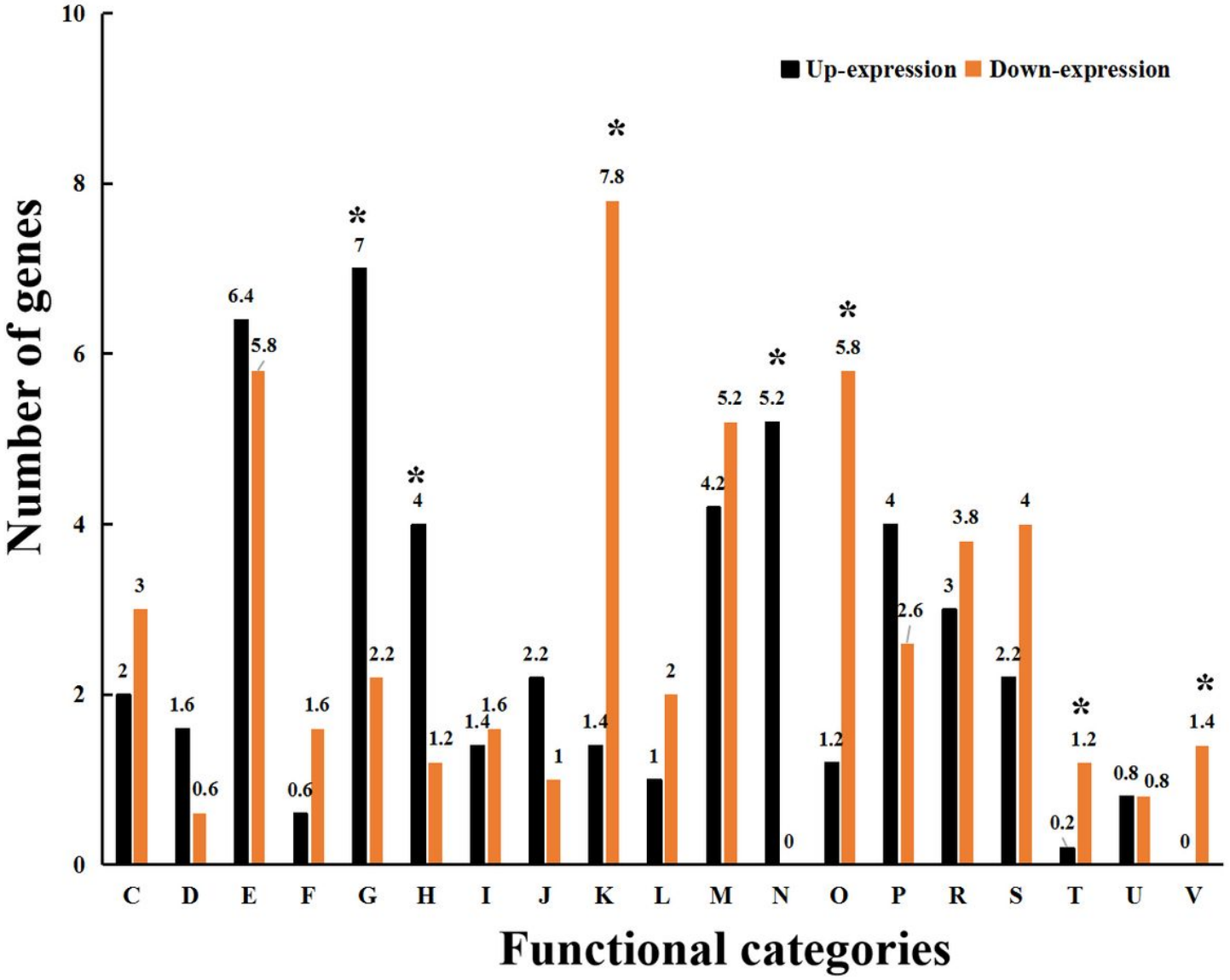

Figure 5

Functional categories of the top 500 differentially expressed genes in A. sinicus nodules infected by the fmoA mutant versus the wild type 7653R. Bars represent the number of up-expression (black) and down-regulated (orange) genes in fmoA mutant bacteroids compared with wild type bacteroids.The number in each bar represents its up/down-expression percentage (%). C: Energy production and conversion; D: Cell cycle control, cell division, chromosome partitioning; E: Amino acid transport and metabolism; F: Nucleotide transport and metabolism; G: Carbohydrate transport and metabolism; H: Coenzyme transport and metabolism; I: Lipid transport and metabolism; J: Translation, ribosomal structure and biogenesis; K: Transcription; L: Replication, recombination and repair; M: Cell wall/membrane/envelope biogenesis; N: Cell motility; O: Posttranslational modification, protein turnover, chaperones; P: Inorganic ion transport and metabolism; R: General function prediction only; S: Function unknown; T: Signal transduction mechanisms; U: Intracellular trafficking, secretion, and vesicular transport; V: Defense mechanisms. The asterisks (*) indicate statistical significance ((>3-fold, p-value < 0.01).

Supplementary Files

This is a list of supplementary files associated with this preprint. Click to download.

- Additionalfile1FigureS1.fmoAmutantrootnoduels.tif
- TableS2.Strainsplasmidsandprimers.docx
- TableS1.fmoAsignificanttop500geneexpression.xlsx